Steric and Electronic Effects in Linkage Isomerization Reactions of $M(CO)_5(L)$ (M = Cr, Mo, W; L = 2-methyl-2,3-dihydrofuran, 2,3-dihydropyran)

A. Shagal and Richard H. Schultz*

Department of Chemistry, Bar-Ilan University, 52900 Ramat-Gan, Israel

Received May 8, 2007

Time-resolved infrared absorption spectroscopy is used to investigate the kinetics of the linkage isomerization reaction $M(CO)_5(\eta^1\text{-L}) \rightarrow M(CO)_5(\eta^2\text{-L})$, where M = Cr, Mo, or W, and L = 2-methyl-2,3-dihydrofuran or 2,3-dihydropyran. Photolysis of $M(CO)_6$ in cyclohexane in the presence of excess L produces the η^1 (O-bound) isomer as the sole kinetic product. The kinetic product subsequently reacts intramolecularly to form an equilibrium mixture of the η^1 and η^2 (C═C bound) isomers. Activation and equilibrium parameters are derived for the reactions and compared with previous results for linkage isomerization of the $M(CO)_5$(dihydrofuran) complexes. The results of the experimental study, supported by DFT calculations, indicate that for M = W the kinetics of the $\eta^1 \rightarrow \eta^2$ isomerization depend primarily on how close the double bond is to the metal atom in the η^1 isomer, while the thermodynamics of the $\eta^1 \rightleftarrows \eta^2$ equilibrium are determined primarily by electronic factors. In contrast, for M = Cr and Mo, both steric and electronic factors play a role in the isomerization kinetics.

Introduction

Two complexes that differ only in the atom through which an ambidentate ligand binds are known as *linkage isomers*.[1] The phenomenon of linkage isomerization was first reported in 1857,[2] and the kinetics of the process continues to be a subject of considerable interest.[3−8] While most research on linkage isomerization has involved complexes that contain inorganic ligands such as NO_2^- and SO_2, the process has been investigated in complexes with organic ligands as well.[4]

In a previous report from our laboratory, we presented an interesting example of $\eta^1 \rightarrow \eta^2$ linkage isomerization.[9,10] When a cyclohexane (CyH) solution of $M(CO)_6$ (M = Cr, Mo, or W) undergoes flash photolysis in the presence of excess 2,3- or 2,5-dihydrofuran (DHF), the sole kinetic product, formed with a room-temperature bimolecular rate constant of $\sim 10^6-10^7$ L mol^{-1} s^{-1}, is $M(CO)_5(\eta^1\text{-DHF})$, in which the ligand is bound to the metal through its oxygen atom. On a significantly longer time scale (ms to s), the η^1 complex undergoes an intramolecular linkage isomerization reaction to form the η^2 structure, in which the ligand is bound to the metal via its double bond, reaction 1, shown here for M = W, L = 2,5-DHF:

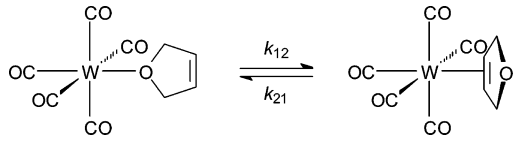

(1)

In general, reaction 1 does not go to completion, but rather to an equilibrium mixture of the two linkage isomers. We found that for the complex containing a given isomer of DHF, K_{eq} (defined as $[M(CO)_5(\eta^2\text{-L})]_\infty/[M(CO)_5(\eta^1\text{-L})]_\infty$) is larger when M = W than it is when M = Cr or Mo, due to the softer metal's greater preference for the π-acceptor ligand. On the other hand, the $\eta^1 \rightarrow \eta^2$ isomerization *rate* proceeds in the order Mo > Cr ≫ W, the usual reactivity order of the group 6 metals. We also found that for a given metal the isomerization is faster for 2,3-DHF than it is for 2,5-DHF. This difference in kinetics is due primarily to differences in $\Delta H^‡$ rather than $\Delta S^‡$ and is apparently a consequence of the smaller amount of rearrangement required for the isomerization when L = η^1-2,3-DHF as well as of the

* To whom all correspondence should be addressed. E-mail: schultr@mail.biu.ac.il. Fax: (+972)-3-738-4053.

(1) Burmeister, J. L.; Basolo, F. *Inorg. Chem.* **1964**, *3*, 1587.

(2) (a) Gibbs, W.; Genth, F. A. *Am. J. Sci.* **1857**, *24*, 86. (b) Werner, A. *Ber.* **1907**, *40*, 765. (c) Basolo, F.; Stone, B. D.; Bergmann, J. G.; Pearson, R. G. *J. Am. Chem. Soc.* **1954**, *76*, 3079.

(3) (a) Fraser, R. T. M. *Adv. Chem. Ser.* **1967**, *62*, 295. (b) Burmeister, J. L. *Coord. Chem. Rev.* **1968**, *3*, 225. (c) Balahura, R. J.; Lewis, N. A. *Coord. Chem. Rev.* **1976**, *20*, 109. (d) Jackson, W. G.; Sargeson, A. M. In *Rearrangements in Ground and Excited States*; de Mayo, P., Ed.; Academic Press: New York, 1980; Vol. 2, p 336. (e) Burmeister, J. L. *Coord. Chem. Rev.* **1990**, *105*, 77. (f) Buckingham, D. A. *Coord. Chem. Rev.* **1994**, *135/136*, 587. (g) Chen, J.; Angelici, R. J. *Coord. Chem. Rev.* **2000**, *206−207*, 63.

(4) (a) Jeong, W.-Y.; Holwerda, R. A. *Inorg. Chem.* **1988**, *27*, 2571. (b) Taube, H. *Pure Appl. Chem.* **1991**, *63*, 651. (c) Ladogana, S.; Nayak, S. K.; Smit, J. P.; Dobson, G. R. *Inorg. Chem.* **1997**, *36*, 650. (d) Keiter, R. L.; Benson, J. W.; Keiter, E. A.; Lin, W.; Jia, Z.; Olson, D. M.; Brandt, D. E.; Wheeler, J. L. *Organometallics* **1998**, *17*, 4291. (e) Cole, S.; Dulaney, K. E.; Bengali, A. A. *J. Organomet. Chem.* **1998**, *560*, 55. (f) Liu, S.; Lucas, C. R.; Newlands, M. J.; Charland, J.-P. *Inorg. Chem.* **2000**, *29*, 4380. (g) Angelici, R. J. *Organometallics* **2001**, *20*, 1259. (h) Kovalevsky, A. Yu.; Bagley, K. A.; Cole, J. M.; Coppens, P. *Inorg. Chem.* **2003**, *42*, 140. (i) To, T. T.; Barnes, C. E.; Burkey, T. J. *Organometallics* **2004**, *23*, 2708.

(5) Powell, D. W.; Lay, P. A. *Inorg. Chem.* **1992**, *31*, 3542.

(6) Quirós Méndez, N.; Seyler, J. W.; Arif, A. M.; Gladysz, J. A. *J. Am. Chem. Soc.* **1993**, *115*, 2323.

(7) Bergamo, M.; Beringhelli, T.; D'Alfonso, G.; Maggioni, D.; Mercandelli, P.; Sironi, A. *Inorg. Chim. Acta* **2003**, *350*, 475.

(8) (a) Kovalevsky, A. Yu.; Bagley, K. A.; Cole, J. M.; Coppens, P. *Inorg. Chem.* **2003**, *42*, 140. (b) Hortalá, M. A.; Fabbrizzi, L.; Foti, F.; Licchelli, M.; Poggi, A.; Zema, M. *Inorg. Chem.* **2003**, *42*, 664. (c) Armstrong, E. A. P.; Brown, R. T.; Sekwale, M .S.; Fletcher, N. C.; Gong, X.-Q.; Hu, P. *Inorg. Chem.* **2004**, *43*, 1714. (d) Bitterwolf, T. E. *J. Photochem. Photobiol. A* **2004**, *163*, 209. (e) Butcher, D. P., Jr.; Rachford, A. A.; Petersen, J. L.; Rack, J. J. *Inorg. Chem.* **2006**, *45*, 9178.

(9) Elgamiel, R.; Huppert, I.; Lancry, E.; Yerucham, Y.; Schultz, R. H. *Organometallics* **2000**, *19*, 2237.

(10) Shagal, A.; Schultz, R. H. *Organometallics* **2002**, *21*, 5657.

10.1021/om700456x CCC: $37.00
Publication on Web 08/23/2007

conjugation of the double bond's π system to the p orbitals of the O atom in 2,3-DHF.[11]

In the present report, we extend our previous work to include $\eta^1 \rightarrow \eta^2$ linkage isomerization of M(CO)$_5$L complexes where L = 2-methyl-2,3-DHF (MeDHF) or 2,3-dihydropyran (DHP). Our choice of these two ligands was motivated by our interest in understanding how changing the electronic and steric properties of the ligand affects the overall reactivity. We chose to study linkage isomerization of M(CO)$_5$(MeDHF) because, on one hand, η^1-MeDHF should be a stronger electron donor than η^1-2,3-DHF, and hence more reactive toward reaction 1, which on the other, the additional steric crowding in the η^1-MeDHF complex might slow the reaction instead. We have observed such competition between steric and electronic factors in the ligand substitution reactions of the transient complex W(CO)$_5$(CyH) with 2-methylfuran and 2,5-dimethylfuran,[12] and Stringfield and Shepherd reported that the preferred coordination geometry of aminopyridines to W(CO)$_5$ (both the kinetic product distribution and the thermodynamically favored linkage isomer) depends on a finely tuned balance of electronic and steric factors.[13] Our study of reaction 1 with L = DHP was motivated by our desire to learn what influence (if any) the size and structure of the C$_n$H$_{2n-2}$O ring have on the kinetics and thermodynamics of the linkage isomerization reaction.

Experimental Section

The apparatus on which these experiments were performed has been described in detail previously,[14] so only a brief description is given here. Reaction takes place in a 0.5 mm path length CaF_2 IR cell, in which a CyH solution containing $(0.5-1) \times 10^{-3}$ mol L^{-1} M(CO)$_6$ and a large excess of L is photolyzed by the pulsed output of a XeCl excimer laser (308 nm, ~20 ns/pulse, typically 60−100 mJ/pulse). The photolysis pulse causes ejection of a CO ligand and formation, within the laser flash,[15] of the solvated complex M(CO)$_5$(CyH). Carbonyl stretching frequencies (ν_{CO}) of this intermediate and any reaction products that appear within ~100 μs of the photolysis flash are determined by time-resolved step-scan FTIR (S^{2}FTIR) spectroscopy. For reaction products that appear on longer time scales, values of ν_{CO} are determined by exposing a solution containing M(CO)$_6$ and excess L in CyH to multiple pulses from the UV laser and then measuring its IR spectrum normally.

Once the relevant IR absorption frequencies have been determined, the isomerization kinetics are measured by using time-resolved IR absorption spectroscopy (TRIR). In this experiment, a CW Pb-salt IR laser is tuned to a frequency corresponding to a C−O stretching absorption of the reactant or product. The laser output, collimated to a ~5 mm beam, passes through the cell collinear with and completely overlapped by the UV laser output, after which it impinges on an InSb (~50 ns rise time) or MCT (<20 ns rise time) detector. The raw signal from the detector is converted into the time-dependent absorbance change ΔA_t. First-order or pseudo-first-order rate constants (k_{obs}) are determined from a linear fit to $\ln|\Delta A_0 - \Delta A_\infty|$.

CyH was obtained in HPLC grade and distilled from Na/benzophenone. The other reagents were obtained from commercial suppliers in purities of >97% (confirmed by ^{1}H NMR for MeDHF and DHP) and used without further purification.

DFT calculations were performed by using the Gaussian 98 suite of programs.[16] Transition states were calculated by using the STQN method; in all cases, the calculation yielded a single negative frequency for the transition state (while in no case did a calculation of a structure corresponding to an energy minimum yield a negative frequency). Most of the calculations were done by using the B3LYP functional with the CEP-31G* basis set for all of the atoms. As described below, in order to check the accuracy of the calculated geometries, additional calculations were performed on the W(CO)$_5$L complexes in which the B3PW91 functional was used instead of the B3LYP, or in which the LANL2DZ basis set[17] was used for the W atom, or in which both changes were made.

Results

General. Qualitatively, the kinetic behavior of the systems studied here follows a similar course to that previously observed for the reactions of M(CO)$_5$(CyH) with DHF. The sole initial kinetic product of the reaction, formed with a rate constant on the order of 10^6 L mol^{-1} s^{-1}, has ν_{CO} corresponding to those of a σ-donor ligand, and we assign to it the structure M(CO)$_5$(η^1-*O*-L). On a longer time scale, this η^1 complex undergoes a further reaction to form a second product, with ν_{CO} similar to those seen in alkene complexes, and to which we assign the structure M(CO)$_5$(η^2-*C*,*C*-L). The η^2 structure of the second product has been confirmed by ^{1}H NMR for W(CO)$_5$(2,5-DHF).[9]

Typical S^{2}FTIR results for the photolysis of a CyH solution containing Cr(CO)$_6$ and excess MeDHF are shown in Figures 1 and 2. The spectra show the disappearance of the Cr(CO)$_5$(CyH) intermediate formed at the flash and the formation of the two linkage isomers of Cr(CO)$_5$(MeDHF), with Cr(CO)$_5$(η^1-MeDHF) appearing during the first 20 μs following the photolysis and formation of Cr(CO)$_5$(η^2-MeDHF) occurring on a time scale of several hundred microseconds.

In Figure 2, the spectra corresponding to absorbances of Cr(CO)$_5$(η^1-MeDHF) appear to decay to zero, and the peak absorbances of the η^2 product are significantly lower than those of the η^1 isomer. These apparent values of ΔA do not reflect the actual kinetics of the reaction, but are rather an artifact of the way the experiment is performed. Under the conditions of

(11) (a) Cram, D. J.; Gosser, L. *J. Am. Chem. Soc.* **1964**, *86*, 2950. (b) Cram, D. J.; Willey, F.; Fischer, H. P.; Scott, D. A. *J. Am. Chem. Soc.* **1964**, *86*, 5370. (c) Houk, K. N. *J. Am. Chem. Soc.* **1973**, *95*, 4092. (d) Wong, S. S.; Paddon-Row, M. N.; Li, Y.; Houk, K. S. *J. Am. Chem. Soc.* **1990**, *112*, 8679. (e) Yoshioka, Y.; Yamada, S.; Kawakami, T.; Nishino, M.; Yamaguchi, K.; Saito, I. *Bull. Chem. Soc. Jpn.* **1996**, *69*, 2683. (f) Pugnaud, S.; Masure, D.; Halle, J.-C.; Chaquin, P. *J. Org. Chem.* **1997**, *62*, 8687. (g) Bonnarme, V.; Bachmann, C.; Cousson, A.; Mondon, M.; Gesson, J.-P. *Tetrahedron* **1999**, *55*, 433.

(12) Krishnan, R.; Schultz, R. H. *Organometallics* **2001**, *20*, 3314.

(13) Stringfield, T. W.; Shepherd, R. E. *Inorg. Chim. Acta* **2003**, *343*, 156.

(14) Paur-Afshari, R.; Lin, J.; Schultz, R. H. *Organometallics* **2000**, *19*, 1682.

(15) (a) Welch, J. A.; Peters, K. S.; Vaida, V. *J. Phys. Chem.* **1982**, *86*, 1941. (b) Simon, J.; Peters, K. S. *Chem. Phys. Lett.* **1983**, *98*, 53. (c) Wang, L.; Zhu, X.; Spears, K. G. *J. Am. Chem. Soc.* **1988**, *110*, 8695. (d) Lee, M.; Harris, C. B. *J. Am. Chem. Soc.* **1989**, *111*, 8963. (e) Xie, X.; Simon, J. D. *J. Phys. Chem.* **1989**, *93*, 4401. (f) Joly, A. G. Nelson, K. A. *Chem. Phys.* **1991**, *152*, 69.

(16) Frisch, M. J.; Trucks, G. W.; Schlegel, H. B.; Scuseria, G. E.; Robb, M. A.; Cheeseman, J. R.; Zakrzewski, V. G.; Montgomery, J. A.; Stratmann, R. E.; Burant, J. C.; Dapprich, S.; Milam, J. M.; Daniels, A. D.; Kudin, K. N.; Strain, M. C.; Farkas, O.; Tomasi, J.; Barone, V.; Cossi, M.; Cammi, R.; Mennucci, B.; Pomelli, C.; Adamo, C.; Clifford, S.; Ochterski, J.; Petersson, G. A.; Ayala, P. Y.; Cui, Q.; Morokuma, K.; Malick, D. K.; Rabuck, A. D.; Raghavachari, K.; Foresman, J. B.; Cioslowski, J.; Ortiz, J. V.; Stefanov, B.; Liu, G.; Liashenko, A.; Piskorz, P.; Komaromi, I.; Gomperts, R.; Martin, R. L.; Fox, D. J.; Keith, T.; Al-Laham, M. A.; Peng, C. Y.; Nanayakkara, A.; Gonzalez, C.; Challacombe, M.; Gill, P. M. W.; Johnson, B. G.; Chen, W.; Wong, M. W.; Andres, J. L.; Head-Gordon, M.; Replogle, E. S.; Pople, J. A. *Gaussian 98* (Revision A.7); Gaussian, Inc.: Pittsburgh, 1998.

(17) (a) Hay, P. J.; Wadt, W. R. *J. Chem. Phys.* **1985**, *82*, 270. (b) The LANL2DZ basis set for W was obtained from the Extensible Computational Chemistry Environment Basis Set Database, Version 02/02/06, as developed and distributed by the Molecular Science Computing Facility, Environmental and Molecular Sciences Laboratory, which is part of the Pacific Northwest Laboratory, P.O. Box 999, Richland, WA 99352, and funded by the U.S. Department of Energy.

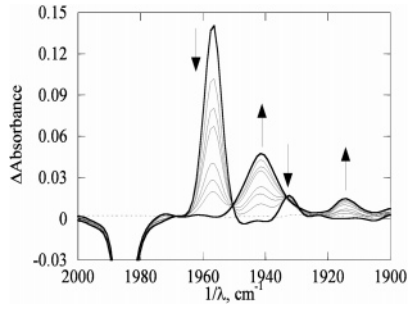

Figure 1. S²FTIR spectra taken 0, 1, 2, 3, 5, 7, 10, and 20 μs following room-temperature photolysis of a CyH solution containing $Cr(CO)_6$ and 0.02 mol L^{-1} MeDHF. The absorbances that appear at the flash and decrease with time (1957 and 1933 cm^{-1}) are attributed to $Cr(CO)_5$(CyH), while those that grow in (1942 and 1914 cm^{-1}) are attributed to $Cr(CO)_5(\eta^1$-MeDHF).

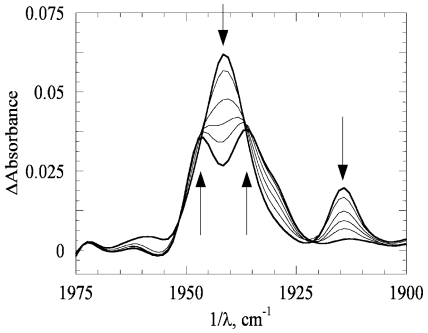

Figure 2. S²FTIR spectra taken 20, 50, 100, 150, 200, and 300 μs after room-temperature photolysis of a CyH solution containing $Cr(CO)_6$ and 0.02 mol L^{-1} MeDHF. The peaks that grow in at 1947 and 1936 cm^{-1} are attributed to $Cr(CO)_5(\eta^2$-MeDHF). The apparent decay of the $Cr(CO)_5(\eta^1$-MeDHF) absorbances to zero is an artifact; see the text.

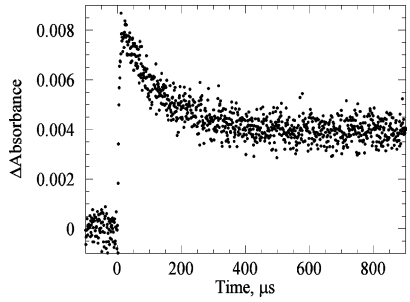

Figure 3. Absorbance change at 1915 cm^{-1}, corresponding to an A_1 C−O stretch of $Cr(CO)_5(\eta^1$-MeDHF), as a function of time following photolysis of a 24 °C CyH solution containing 5.6×10^{-4} mol L^{-1} $Cr(CO)_6$ and 0.024 mol L^{-1} MeDHF.

the step-scan experiment, the solution flows continuously through the cell so that each photolysis pulse of the laser irradiates fresh solution. That means that for any kinetic process that is sufficiently slow, unphotolyzed solution will enter the cell, and molecules that have been exposed to the photolysis laser will leave it, before the reaction has gone to completion. The measured ΔA thus declines, not due to reaction, but due to physical replacement of $M(CO)_5$(L) with $M(CO)_6$. This process presumably explains the apparent lack of an isosbestic point in the S²FTIR spectra, since the measured ΔA's for the η^2 complex also begin to decline as $M(CO)_5(\eta^1$-L) is carried out of the path of the IR beam.

Figure 3 shows a TRIR trace of the decay of the $Cr(CO)_5(\eta^1$-MeDHF) absorbance at 1915 cm^{-1}. In this experiment, the photolysis laser operates at a much slower repetition rate (0.4 Hz instead of ~6 Hz), and the solution flows through the cell only during the dead time when no TRIR measurement is being made. As is apparent from the figure, the amount of $Cr(CO)_5(\eta^1$-MeDHF) decays to a constant but nonzero value over a few hundred microseconds at room temperature, indicating that the final "product" is an equilibrium mixture of the two isomers.

In our previous report,[10] we showed how the forward and reverse rate constants for reaction 1 (k_{12} and k_{21}, respectively) and the equilibrium constant K_{eq} of the final product mixture can be derived from measurements of k_{obs}, the observed first-order rate constant for the $\eta^1 \rightarrow \eta^2$ isomerization ($k_{obs} = k_{12} + k_{21}$), and $\Delta A_\infty/\Delta A_0$ ($=K_{eq}$). The same procedure was used here to derive the reported values of k_{12} and K_{eq}.[18] These values, along with the experimentally measured values of k_{obs} and $\Delta A_\infty/\Delta A_0$ from which they were derived, are given in Tables S-1 through S-6 of the Supporting Information.

In some cases, $\Delta A_\infty/\Delta A_0$ was found to depend on [L] even though k_{obs} itself did not. As explained in our previous report, we believe that this result is due to interference from residual H_2O in the solution rather than any involvement of a second molecule of L in the isomerization process or decomposition of $M(CO)_5$(L). Because of the output characteristics of the diode laser in our laboratory, the only C−O stretch of $M(CO)_5(\eta^1$-L) that is accessible as a spectroscopic probe for TRIR study in our instrument is the $A_1(2)$ vibration, which is found at 1910−1915 cm^{-1}, Table 1. This wavelength happens to be near that of the $A_1(2)$ C−O stretch of $M(CO)_5(H_2O)$.[19] At low [L], traces of H_2O in the solution can compete with L for the $M(CO)_5$(CyH) intermediate formed in the initial photolysis of $M(CO)_6$. Since $M(CO)_5(H_2O)$ is formed much more rapidly from $M(CO)_5$(CyH) than $M(CO)_5(\eta^2$-L) is formed from $M(CO)_5(\eta^1$-L), and since $M(CO)_5(H_2O)$ is stable on the time scale of the linkage isomerization reaction, fast production of $M(CO)_5(H_2O)$ will produce a nonzero baseline in the time-dependent IR absorption measurement made at 1910−1915 cm^{-1} over time scales longer than that of the formation of $M(CO)_5(H_2O)$. This nonzero baseline will then produce a spuriously high value for $\Delta A_\infty/\Delta A_0$ and consequently a spuriously low value of K_{eq}.[20] At high [L], the residual H_2O cannot compete as efficiently for the $M(CO)_5$(CyH) intermediate, so the effect of this baseline on $\Delta A_\infty/\Delta A_0$ is much less significant. Therefore, we report only measurements of k_{obs} (and k_{12} and K_{eq} calculated therefrom) made at [L] high enough that $\Delta A_\infty/\Delta A_0$ is independent of [L] to within experimental error.

There is one additional possible cause of error in our determinations of the rate and equilibrium constants that needs to be considered.[21] At high concentrations of [L], the solvation shell of unphotolyzed $M(CO)_6$ should contain a significant amount of L (2 mol L^{-1} ligand represents a concentration of ~20% by volume). Thus, given the tendency of "naked" $M(CO)_5$ not to discriminate among possible reaction partners,[15] there might be prompt (picosecond) formation of $M(CO)_5(\eta^2$-L) in addition to $M(CO)_5$(CyH) and $M(CO)_5(\eta^1$-L). If prompt formation of $M(CO)_5(\eta^2$-L) were occurring, then our derived values of the equilibrium and rate constants would be affected,

(18) Note that since only two parameters (k_{obs} and $\Delta A_\infty/\Delta A_0$) are measured independently, we can determine only two of the three parameters k_{12}, k_{21}, and K_{eq} independently. As described in our previous report, we define $k_{21} \equiv k_{12}/K_{eq}$.

(19) Hermann, H.; Grevels, F.-W.; Henne, A.; Schaffner, K. *J. Phys. Chem.* **1982**, *86*, 5151.

(20) Note that on the time scale of the isomerization, k_{obs}, which depends only on $d\Delta A/dt$, remains independent of [L] even in the presence of a nonzero baseline.

(21) We thank one of the reviewers of the manuscript for bringing this point to our attention.

Table 1. C−O Stretching Frequencies and Force Constants[a] for M(CO)$_5$(L)

		M(CO)$_5$(η^1-L)						M(CO)$_5$(η^2-L)					
		ν_{CO}, cm^{-1}			force constant, 10^2 N m^{-1}			ν_{CO}, cm^{-1}			force constant, 10^2 N m^{-1}		
M	L	$A_1(1)$	E	$A_1(2)$	k_t	k_c	k_i	$A_1(1)$	E	$A_1(2)$	k_t	k_c	k_i
Cr	2,3-DHF[b]	2075	1943	1915	15.028	15.893	0.321	2069	1954	1945	15.468	15.984	0.280
	DHP	2074	1942	1915	15.028	15.877	0.321	2069	1952	1932	15.268	15.962	0.285
	MeDHF	2076	1941	1914	15.018	15.876	0.329	2063	1947	1936	15.329	15.877	0.282
Mo	2,3-DHF[b]	2077	1947	1916	15.041	15.947	0.317	2077	1961	1941	15.408	16.102	0.284
	DHP	2078	1947	1914	15.012	15.952	0.319	2076	1960	1933	15.283	16.086	0.284
	MeDHF	2076	1946	1913	14.994	15.931	0.317	2074	1952	1933	15.292	15.987	0.298
W	2,3-DHF[b]	2075	1934	1913	15.011	15.794	0.343	2077	1957	1940	15.399	16.058	0.293
	DHP	2078	1936	1913	15.013	15.831	0.345	2069	1953	1934	15.298	15.973	0.283
	MeDHF	2078	1936	1912	14.998	15.831	0.345	2072	1946	1932	15.283	15.911	0.307

[a] k_t, force constant for carbonyl trans to L; k_c, force constant for carbonyl cis to L; k_i, interaction force constant for mutually cis carbonyls. Force constants determined by using the Cotton−Kraihanzel method (Cotton, F. A.; Kraihanzel, C. S. *J. Am. Chem. Soc.* **1962**, *84*, 4432). [b] Ref 10.

since their derivation assumes that [M(CO)$_5$(η^2-L)]$_0$ = 0. We cannot rule out this possibility entirely, due to spectral overlap between the absorbances of M(CO)$_5$(η^2-L) and those of either M(CO)$_5$(η^1-L) or of M(CO)$_5$(CyH) (Table 1). Because of this spectral overlap, at t = 0, there will be an increase in absorbance at frequencies corresponding to C−O stretches of M(CO)$_5$(η^2-L) whether or not it is formed at the laser flash.

Several pieces of evidence indicate, however, that prompt formation of M(CO)$_5$(η^2-L) is *not* occurring in our experiments to any significant extent. First of all, S^{2}FTIR spectra taken at high [L] do not show any evidence for prompt formation of M(CO)$_5$(η^2-L), but do show prompt formation of M(CO)$_5$(η^1-L) and clean pseudo-first-order conversion of M(CO)$_5$(CyH) to M(CO)$_5$(η^1-L) (see Figure S-5 of the Supporting Information). In addition, as described in the paragraph above, and shown below, once [L] is high enough to suppress competition with formation of M(CO)$_5$(H$_2$O), there is no correlation between [L] and the derived values of K_{eq}, contrary to what would be expected if significant amounts of M(CO)$_5$(η^2-L) were being formed at the laser flash. We note as well a study by Dobson and co-workers[4c] of the linkage isomerization of Cl-bound Cr(CO)$_5$(η^1-5-chloropent-1-ene), created by flash photolysis of Cr(CO)$_6$ in a solution containing excess ligand, to the π-bound η^2 isomer. The time-dependent spectra shown in that report fail to show any evidence for prompt formation of the η^2 isomer. Experiments such as ours and those performed by Dobson and co-workers cannot unambiguously determine why the η^2 isomer is not formed at the laser flash. It seems that either the ligand solvates unphotolyzed M(CO)$_6$ with the σ-donating atom directed toward the complex, leading to prompt formation only of the η^1-linkage isomer (since naked M(CO)$_5$ tends to bind to the first atom of the solvent molecule that it encounters[15]), or there is a barrier to formation of the η^2 isomer even from "naked" M(CO)$_5$ that precludes its formation on a picosecond time scale.

To test whether the reaction we observed is truly intramolecular, for each reaction, we performed the kinetic measurements at different concentrations of M(CO)$_6$ (varying by a factor of 2) and of L (varying by a factor of ~100). We found k_{obs}, and to within the limitations discussed in the previous paragraph, k_{12}, to be independent of the concentration of either the metal or the ligand. We take the independence of the rate constant on reactant concentration to mean that the reaction is indeed intramolecular linkage isomerization.

DHP. An Eyring analysis of the forward isomerization rate constant k_{12} is shown in Figure 4 for isomerization of M(CO)$_5$(η^1-DHP) and includes various values of [M] and [DHP] as described above.

Over the temperature range studied here, k_{12} for reaction 1 (L = DHP) decreases in the order Mo > Cr > W, while for a given metal, k_{12} decreases in the order DHP > 2,3-DHF > 2,5-DHF.[10] Activation parameters for the isomerization reactions are summarized in Table 2.

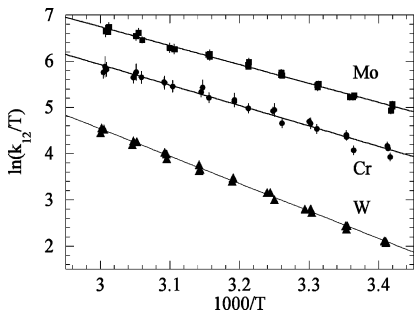

Figure 4. Eyring analyses of k_{12} for reaction 1 with L = DHP and M = Cr (●), Mo (■), and W (▲). The solid lines represent least-squares linear fits to the data points, and the error bars are 1σ uncertainties in the values of k_{12}.

Table 2. Eyring Activation Parameters for Reaction 1 (1σ uncertainties in parentheses)

ligand	metal	$\Delta H^{\ddagger}$, kcal mol^{-1}	$\Delta S^{\ddagger}$, eu	k_{12}(300 K), 10^3 s^{-1}
2,3-DHF[a]	Cr	13.7 (0.3)	4.0 (1.1)	4.9
	Mo	11.2 (0.4)	−2.2 (2.1)	14
	W	13.3 (0.2)	−1.2 (0.9)	0.70
DHP	Cr	10.5 (0.4)	−2.5 (1.2)	40
	Mo	9.2 (0.2)	−5.3 (0.5)	86
	W	12.2 (0.2)	−1.0 (0.7)	4.9
MeDHF	Cr	10.4 (0.2)	−6.9 (0.7)	5.2
	Mo	11.4 (0.2)	−3.9 (0.7)	4.4
	W	14.0 (0.2)	1.1 (0.7)	0.23

[a] Ref 10.

A van't Hoff plot of K_{eq} for isomerization of Cr(CO)$_5$(η^1-DHP) is given in Figure 5. Analogous plots for the Mo and W complexes are given in Figures S-1 and S-3 of the Supporting Information. Equilibrium thermodynamic parameters are summarized in Table 3.

The three data sets shown in Figure 5 appear to give systematically different values for the equilibrium thermodynamic parameters; in particular, the values of K_{eq} derived from rate constants measured at [Cr(CO)$_6$] = 1.0 × 10^{-3} mol L^{-1} and [DHP] = 0.2 mol L^{-1} seem to diverge from the others. The scatter in the data and the uncertainties in the individual values of K_{eq} are sufficiently large, however, that ΔH° and ΔS° derived from any individual data set are within combined experimental error of those derived from the average of all of the data sets. Similar behavior (i.e., systematically different values of K_{eq} from different data sets) was observed in some (but not all) of the other reactions systems as well (see Figures S-1 through S-4 of the Supporting Information). There do not appear to be anysystematic trends in the derived values of K_{eq}

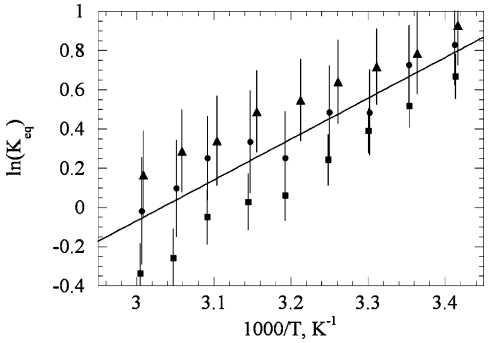

Figure 5. van't Hoff plot for the linkage isomerization of $Cr(CO)_5$(DHP). Shown are values for K_{eq}, derived as described in the text, for solutions containing (prior to photolysis) 5×10^{-4} mol L^{-1} $Cr(CO)_6$ and 0.2 mol L^{-1} DHP (●); 1.0×10^{-3} mol L^{-1} $Cr(CO)_6$ and 0.2 mol L^{-1} DHP (■); and 5×10^{-4} mol L^{-1} $Cr(CO)_6$ and 2.0 mol L^{-1} DHP (▲). The solid line is a least-squares fit to all of the data points shown. Error bars are 1σ uncertainties in the estimates of K_{eq}.

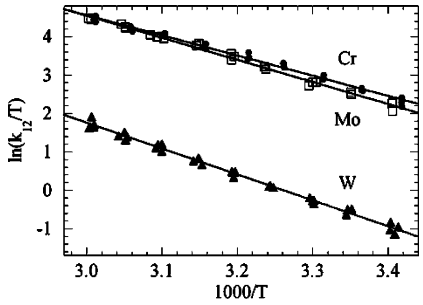

Figure 6. Eyring analyses of the rate constant k_{12} of reaction 1 with L = MeDHF for M= Cr (●), Mo (□), and W (▲). The lines represent least-squares fits to the data.

Table 3. Equilibrium Parameters for Reaction 1 (1σ uncertainties in parentheses)

ligand	metal	$\Delta H°$, kcal mol^{-1}	$\Delta S°$, eu	K_{eq}, 300 K
2,3-DHF[a]	Cr	−2.4 (0.5)	−4.5 (1.5)	5.8 (1.1)
	Mo	−1.2 (0.6)	−1.3 (2.1)	3.9 (1.5)
	W	−0.9 (0.4)	1.2 (1.3)	8.3 (0.9)
DHP	Cr	−4.1 (0.5)	−12.6 (1.6)	1.7 (1.1)
	Mo	−3.0 (0.3)	−8.2 (1.1)	2.5 (0.7)
	W	−1.8 (0.4)	−3.2 (1.4)	4.1 (1.0)
MeDHF	Cr	−3.9 (0.3)	−12.5 (1.1)	1.3 (0.7)
	Mo	−3.2 (0.3)	−9.1 (0.8)	2.2 (0.6)
	W	−2.3 (0.1)	−5.1 (0.3)	3.6 (0.2)

[a] Ref 10.

as a function of $[Cr(CO)_6]$ or [L] in the originally prepared solution that would enable us to exclude data sets obtained under any particular set of experimental conditions, however. Furthermore, the values of the *rate constants* were always consistent for all of the measurements made of a particular reaction system. Given that the values of $\Delta H°$ and $\Delta S°$ derived from individual data sets were always within experimental error of the those derived from all of the data taken together, that we have no reason for being able to exclude any specific data set, and that the qualitative conclusions we reach below are not affected by the choice of data sets for a given reaction system, we report equilibrium thermodynamic parameters based on values of K_{eq} derived from all data sets with [L] ≥ 0.2 mol L^{-1}.

MeDHF. Eyring analyses of k_{12} for reaction with MeDHF are shown in Figure 6, and activation parameters summarized in Table 2. Uniquely among the linkage isomerization reactions of $M(CO)_5$(L) that we have studied, and unusually for any reaction of group 6 complexes, for L = MeDHF, the Mo complex is *not* always the most reactive of the three. As shown in Figure 6, Cr and Mo show similar reactivities, with k_{12} (and k_{obs}, Tables S-2 and S-4) actually higher for Cr at temperatures below ∼50 °C.

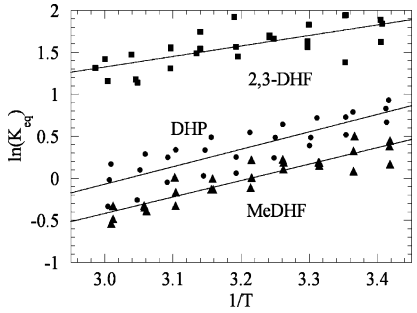

Figure 7. van't Hoff plots for the linkage isomerization of $Cr(CO)_5$(DHP) (●), $Cr(CO)_5$(MeDHF) (▲), and $Cr(CO)_5$(2,3-DHF) (■, ref 10).

For M = Mo or W, k_{12} is much lower for isomerization of $M(CO)_5(\eta^1$-MeDHF) than for $M(CO)_5(\eta^1$-2,3-DHF) over the entire temperature range studied here. For Cr, on the other hand, the relative temperature dependences of reaction 1 for the two systems are markedly different: below ∼30 °C, k_{12} is higher for isomerization of $Cr(CO)_5(\eta^1$-MeDHF), but above this temperature, k_{12} is higher for isomerization of $Cr(CO)_5(\eta^1$-2,3-DHF). These unusual results are discussed in detail below.

Figure 7 shows a van't Hoff plot for the equilibrium constants of the various $Cr(CO)_5$(L) systems. van't Hoff plots for the $Mo(CO)_5$(MeDHF) and $W(CO)_5$(MeDHF) equilibria are given in Figures S-2 and S-4 of the Supporting Information. For all three metals, over the temperature range studied, K_{eq} as a function of L follows the same trend, 2,3-DHF > DHP ∼ MeDHF. Equilibrium thermodynamic parameters are given in Table 3.

Discussion

Kinetics. 1. $M(CO)_5$(DHP). As noted above, for a given metal M, $M(CO)_5(\eta^1$-DHP) isomerizes more rapidly than does $M(CO)_5(\eta^1$-2,3-DHF) over the entire temperature range studied here (20−60 °C). The results summarized in Table 2 indicate that the difference in reactivity is enthalpic. From the IR spectra (Table 1), DHP does not appear to be a significantly better electron donor than 2,3-DHF, implying that the difference in the kinetic behavior of the two ligands is *not* due to differences in electron density at the metal. In our previous study,[10] we argued that the lower $\Delta H^{\ddagger}$ for isomerization when L = 2,3-DHF relative to L = 2,5-DHF is due primarily to the smaller amount of rearrangement necessary to bring the complex from the η^1 to the η^2 geometry. Calculated geometries (B3LYP functional, CEP-31G* basis set on all atoms) for $W(CO)_5(\eta^1$-L), $W(CO)_5(\eta^2$-L), and the transition state that connects them are shown in Figure 8. Additional views are given in Figures S-6 and S-7 of the Supporting Information.

Calculated atom−atom distances (M−O, $M-C_2$, C_2-C_3) for $W(CO)_5$(L) and $Cr(CO)_5$(L) along with calculated activation parameters for $W(CO)_5(\eta^1$-L) are summarized in Table 4. These calculations predict that C_2 (the double bond C atom closer to the W atom in the η^1 complex) is closer to the metal atom for L = DHP than it is for L = 2,3-DHF or MeDHF and that the η^1-DHP complex requires less rearrangement to form the η^2 isomer than does the η^1-2,3-DHF complex: the $W-O-C_2-C_3$ dihedral angle is 172.5° in $W(CO)_5(\eta^1$-2,3-DHF) but only 147.3° in $W(CO)_5(\eta^1$-DHP). In order to double check that the trends in the predicted geometries were not due to the particular

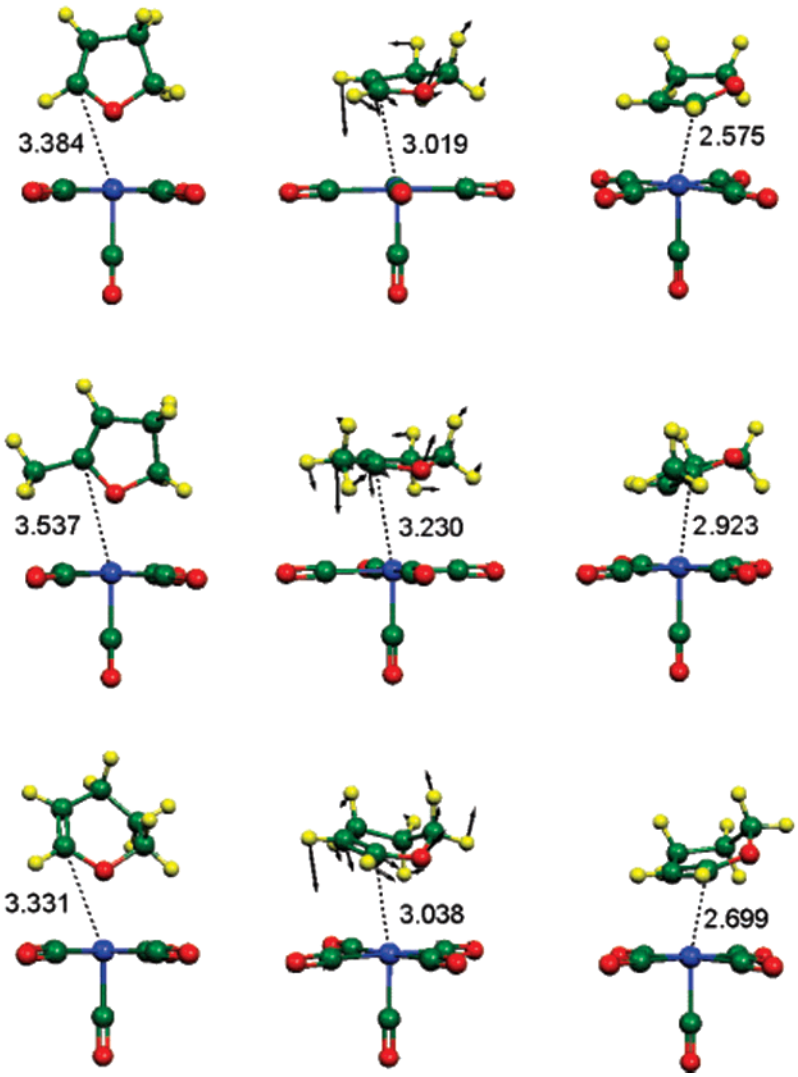

Figure 8. DFT-calculated structures (B3LYP functional, CEP-31G* basis set) for W(CO)$_5$(η^1-L) (left column), W(CO)$_5$(η^2-L) (right column), and the transition state between them (center column), for L = 2,3-DHF (top row), MeDHF (center row), and DHP (bottom row). For each complex, the calculated W−C$_2$ distance is given in Å. The arrows show the relative motions of the atoms along the reaction coordinate at the transition state.

functional and basis set chosen, additional calculations of the W(CO)$_5$(η^1-L) and W(CO)$_5$(η^2-L) complexes were performed using the B3PW91 functional instead of the B3LYP or the LANL2DZ basis set for W instead of CEP-31G*, or both. The results of these calculations are also summarized in Table 4. The same qualitative trend in the W−C$_2$ distance is predicted independent of the choice of functional or basis set. As can be seen in Figure 8 (as well as in Figures S-6 and S-7 of the Supporting Information), the DFT calculations indicate that the isomerization proceeds by direct motion of the metal atom along the face of the ring from the η^1 to the η^2 structure, with the transition state near the midpoint of the rearrangement, rather than by a more dissociative process during which metal−ligand bonding is largely disrupted. The calculations thus support our hypothesis that $\Delta H^{\ddagger}$ of reaction 1 is determined primarily by the amount of rearrangement necessary to effect the isomerization: the closer the η^1 complex is to the η^2 geometry, the less rearrangement is needed to bring the complex to the transition state for the isomerization, and hence the lower the $\Delta H^{\ddagger}$ of reaction 1 will be.

For Cr and Mo, $\Delta S^{\ddagger}$ is significantly lower for isomerization of the DHP complex than it is for isomerization of the 2,3-DHF complex, while for W, the activation entropies are the same to within experimental error. We have previously observed[12] that in ligand substitution reactions at W(CO)$_5$(CyH) by 2-methyl and 2,5-dimethyl derivatives of THF and furan increased steric hindrance manifests itself as an anticorrelation between $\Delta H^{\ddagger}$ and $\Delta S^{\ddagger}$ (i.e., $\Delta S^{\ddagger}$ decreases with increasing $\Delta H^{\ddagger}$). The results of the present experiments are consistent with an analogous steric effect that requires the ligand to be further from the metal center at the transition state in the W complexes, increasing the activation entropy.

2. M(CO)$_5$(MeDHF). While a single explanation appears to account for the kinetic behavior of M(CO)$_5$(η^1-DHP) relative to that of M(CO)$_5$(η^1-2,3-DHF) for all three metals, the kinetics of the isomerization of the η^1-MeDHF complexes do not appear to be so simply rationalized. Figure 9 shows comparative Eyring analyses of k_{12} for linkage isomerization of 2,3-DHF and MeDHF complexes of Cr(CO)$_5$ and W(CO)$_5$.

As can be seen in the figure and summarized in Table 2, for M = Cr, both $\Delta H^{\ddagger}$ and $\Delta S^{\ddagger}$ are lower for isomerization of the MeDHF complex than for the 2,3-DHF complex, so that below ~30 °C the isomerization proceeds faster in the MeDHF complex, while at higher temperatures, the relative reactivity reverses. For M = Mo (not shown in the figure) and W, $\Delta H^{\ddagger}$ is higher for isomerization of the MeDHF complex than it is in

Table 4. Calculated Atom−Atom Distances (Å) and 298.15 K Thermochemistry

		η^1			η^2			$\eta^1 \rightarrow \eta^2$					
functional, basis set	complex	M−O	M−C_2	C_2−C_3	M−O	M−C_2	C_2−C_3	$\Delta H^{\ddagger}$, kcal mol^{-1}	$\Delta S^{\ddagger}$, eu	$\Delta G^{\ddagger}$, kcal mol^{-1}	$\Delta H°$, kcal mol^{-1}	$\Delta S°$, eu	$\Delta G°$, kcal mol^{-1}
	$Cr(CO)_5$(DHF)	2.246	3.282	1.354	3.459	2.631	1.387				−3.34	−6.32	−1.46
	$Cr(CO)_5$(DHP)	2.280	3.238	1.359	3.522	2.678	1.385				−1.08	−4.66	+0.31
B3LYP,	$Cr(CO)_5$(MeDHF)	2.302	3.450	1.358	3.654	2.887	1.393				−4.15	−6.03	−2.35
CEP-31G*	$W(CO)_5$(DHF)	2.352	3.384	1.353	3.414	2.575	1.395	11.6	−1.21	12.0	−4.43	−6.14	−2.59
on all atoms	$W(CO)_5$(DHP)	2.381	3.331	1.358	3.531	2.699	1.394	10.0	−4.16	11.2	−2.85	−5.97	−1.07
	$W(CO)_5$(MeDHF)	2.395	3.537	1.358	3.689	2.923	1.402	12.0	−1.81	12.6	−5.28	−5.96	−3.51
B3PW91,	$W(CO)_5$(DHF)	2.332	3.359	1.352	3.445	2.600	1.401				−9.50	−7.24	−6.93
CEP-31G*	$W(CO)_5$(DHP)	2.357	3.295	1.356	3.446	2.606	1.399				−6.12	−6.36	−4.23
on all atoms	$W(CO)_5$(MeDHF)	2.365	3.503	1.357	3.589	2.815	1.404				−8.52	−7.00	−6.43
B3LYP,	$W(CO)_5$(DHF)	2.324	3.319	1.364	3.380	2.545	1.430				+2.55	−7.20	+4.70
LANL2DZ on W,	$W(CO)_5$(DHP)	2.362	3.266	1.367	3.459	2.614	1.419				+1.24	−5.32	+2.83
CEP-31G* on H, C, O	$W(CO)_5$(MeDHF)	2.348	3.429	1.370	3.493	2.752	1.428				+4.04	−7.32	+6.22
B3PW91	$W(CO)_5$(DHF)	2.294	3.289	1.362	3.317	2.467	1.440				−2.52	−8.34	−0.03
LANL2DZ on W,	$W(CO)_5$(DHP)	2.327	3.232	1.365	3.386	2.521	1.428				−3.02	−6.23	−1.17
CEP-31G* on H, C, O	$W(CO)_5$(MeDHF)	2.313	3.392	1.368	3.376	2.614	1.439				+0.37	−0.47	+0.51

the 2,3-DHF complex, while $\Delta S^{\ddagger}$ is near zero for both reactions (Table 2), so k_{12} is greater for isomerization of the 2,3-DHF complex over the entire temperature range studied here.

The calculated structure of $W(CO)_5(\eta^1$-MeDHF) is given above in Figure 8. The calculation predicts that the M−C_2 distance is larger in the MeDHF complex than it is in either of the other two η^1 complexes, so according to the arguments made above, the isomerization would be expected to be slowest in the MeDHF complex. For Mo and W, this is indeed the case. For $Cr(CO)_5$(L), however, although the DHP complex is the most reactive, the MeDHF results demonstrate that the geometry alone cannot account for the relative isomerization rates. It appears, rather, that there is an electronic effect that competes with the geometrical considerations. As shown in Table 1, the *trans* C−O stretching force constant is significantly lower in $M(CO)_5(\eta^1$-MeDHF) than it is in $M(CO)_5(\eta^1$-2,3-DHF) or $M(CO)_5(\eta^1$-DHP), indicating that, as expected, MeDHF is the strongest electron donor of the three ligands due to the inductive effect of the methyl group. It thus appears that in the case of Cr the relative reactivity is determined not only by the geometry of the η^1 complex but by the relative electron richness of the ligand. Indeed, for Cr, $\Delta H^{\ddagger}$ of reaction 1 is lower for L = MeDHF than it is for L = 2,3-DHF, while for Mo, $\Delta H^{\ddagger}$ is the same to within experimental error in the two cases, and for W, $\Delta H^{\ddagger}$ is higher for isomerization of the MeDHF complex, indicating that as the metal atom gets larger, the electronic effect becomes less important. Furthermore, $\Delta S^{\ddagger}$ of reaction 1 is significantly lower for L = MeDHF only in the case of M = Cr, and of all of the examples of reaction 1 that we have studied, only for L = MeDHF is $\Delta H^{\ddagger}$ *not* lowest for M = Mo. These results are thus consistent with a contribution to the reactivity from steric hindrance. This contribution is least significant for Cr, the smallest of the three metal atoms. We have previously pointed out that an analogous steric effect can explain the differences in $\Delta S^{\ddagger}$ in the associative ligand substitution reactions of $W(CO)_5$(CyH) and $Cr(CO)_5$(CyH).[22]

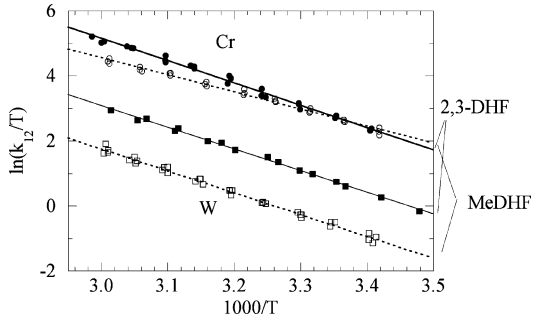

Figure 9. Eyring analyses of k_{12} for $Cr(CO)_5$(L) (●, ○) and $W(CO)_5$(L) (■, □) for L = 2,3-DHF (●, ■, solid lines) and L = MeDHF (○, □, dashed lines). Data for the 2,3-DHF complexes are taken from ref 10. The lines are least-squares linear fits to the data points.

For all three metals, at 300 K, k_{12} is roughly an order of magnitude faster for L = DHP than it is for L = MeDHF. For Mo and W, the difference appears to be enthalpic, while for Cr, the difference appears to have an entropic origin. This difference can be explained by a tighter transition state for isomerization of $Cr(CO)_5$(MeDHF) than for the other two metals, which would both keep the metal more electron rich at the transition state and would provide a more ordered transition state. Thus, comparison of the MeDHF and DHP isomerization kinetics provides further support for our hypothesis that for Mo and W the kinetics are primarily controlled by geometrical considerations, while for Cr, electronic factors (which in this case oppose the geometrical factors) are significant.

In our previous report, we had found that the linkage isomerization of $M(CO)_5(\eta^1$-2,3-DHF) is invariably faster than that of $M(CO)_5(\eta^1$-2,5-DHF) and that the difference in that case was enthalpic for all three metals. We argued in that case that the primary effect seemed to have been geometrical, since the isomerization of the 2,5-DHF complex requires the metal atom to travel across the face of the ligand ring. We could not rule out an electronic effect, however. If reaction 1 proceeds by a "conducted tour" mechanism,[23] then the p−π conjugation of the O atom and the double bond in 2,3-DHF should facilitate the isomerization. The present results tend to cast doubt on that possibility, however, as the p−π conjugation is stronger in 2,3-DHF and MeDHF than it is in DHP,[24] due to the greater planarity of the five-membered rings. As shown in Figure 8, the DHP ligand is expected to be the least planar of the three ligands even in the complex, demonstrating that the ligand with the most p−π conjugation in fact does *not* isomerize most rapidly.

***K*$_{eq}$ and Thermodynamics**. The experimental equilibrium parameters for reaction 1 are summarized in Table 3. The present results are similar in many ways to those that we previously

(22) Biber, L.; Revzin, T.; Reuvenov, D.; Sinai, T.; Zahavi, A.; Schultz, R. H. *Dalton Trans.* **2007**, 41.

(23) (a) Cram, D. J.; Gosser, L. *J. Am. Chem. Soc.* **1964**, *86*, 2950. (b) Cram, D. J.; Willey, F.; Fischer, H. P.; Scott, D. A. *J. Am. Chem. Soc.* **1964**, *86*, 5370.

(24) (a) Taskinen, E. *Tetrahedron* **1978**, *34*, 433. (b) Taskinen, E.; Ora, M. *Magn. Reson. Chem.* **1995**, *33*, 239.

reported for 2,3-DHF and 2,5-DHF. In all cases, the $\eta^1 \rightarrow \eta^2$ isomerization is exothermic, and $\Delta H°$ is much smaller than $\Delta H^‡$ for the reaction. At 300 K, the equilibrium favors the η^2 structure for all of the complexes studied here, with K_{eq}'s of similar magnitude to those reported for $\eta^1 \rightleftarrows \eta^2$ linkage isomerization of aldehyde[6] and ketone[5,7] ligands. To the best of our knowledge, there have not been many reports in the literature of complexes of cyclic enol ethers. Binding of the ligand through the double bond has been observed in such complexes as Cp*Rh(PMe$_3$)-(2,3-DHF)[25] and CpFe(CO)$_2$(L)$^+$ (L = 2,3-DHF or DHP);[26] reaction of the free double bond of η^2-coordinated furan produces a DHF derivative that retains the η^2 coordination;[27] and ring opening of 2,3-DHF by TpRu(CO)(NCMe)(Ph) has been proposed to proceed via an η^2 intermediate.[28] In none of these studies was the issue of linkage isomerization of the enol ether ligand explored, however.

For a given metal, K_{eq} at 300 K follows the order DHP $\sim$ MeDHF < 2,3-DHF. As can be seen from the results summarized in Table 3, this order opposes the order of relative exothermicities of the reactions, indicating that there is a significant entropic effect. One reasonable way of explaining this trend is that relative to the η^1-2,3-DHF complexes, the η^1-DHP and η^1-MeDHF complexes have additional degrees of freedom (and hence additional entropy) in the form of low-frequency vibrations and hindered rotations, due in the former case to the expansion of the ring and in the latter to replacement of a hydrogen atom with a methyl group. Since each ligand is more tightly bound in the η^2 isomer than in the η^1 isomer (i.e., the isomerization is exoenergetic, Table 3), these low-frequency motions will be more restricted in the η^2 complex than in the η^1, leading to greater entropy loss and lowering K_{eq} relative to that of M(CO)$_5$(2,3-DHF). Similar entropic effects have been previously observed in the reactions of alkane-solvated transition metal intermediates.[14,29]

For a given *ligand*, over the temperature range studied here, K_{eq} increases in the order Cr $\lesssim$ Mo < W, the same order we previously observed for isomerization of the 2,3-DHF and 2,5-DHF complexes.[30] Qualitatively, this trend reflects the thermodynamic preference of a softer metal for the softer η^2 isomer. The results summarized in Table 3 indicate that the trend in K_{eq} appears to oppose the trend in $\Delta H°$; that is, K_{eq} is actually largest for the *least* exothermic isomerization. Apparently, as with the kinetics, the thermodynamics represents a balance between electronic and steric factors. For example, our calculations (Table 4) predict that the C=C double bond lengthens more (by $\sim$0.1 A) upon isomerization of W(CO)$_5$(η^1-L) than it does upon isomerization of Cr(CO)$_5$(η^1-L), similar to previous calculations of M(CO)$_5$(η^2-alkene) complexes that had predicted the C=C bond to be longer in the W complex,[31] due to better orbital overlap.[31b] This additional bond lengthening should lead to a greater lowering of the C−C stretching frequency in the W complex, partially compensating for the entropy loss due to the loss of low-frequency M−L modes in the $\eta^1 \rightarrow \eta^2$ isomerization. According to our calculations, the M−L bond distance is shorter for the Cr complexes than it is for the W complexes; it is possible that the steric hindrance in the latter case makes the isomerization less exothermic for the complex containing the larger transition metal atom, similar to the steric effect on the kinetics in which $\Delta H^‡$ is higher for the larger metal atom.[32]

Conclusions

Our observations of the kinetics of the linkage isomerization of M(CO)$_5$(η^1-L) (M = Cr, Mo, W; L = a cyclic ligand containing an O atom and a C=C double bond) lead us to the following conclusions.

Kinetics. Over the temperature range 20−60 °C, the reactivity of complexes as a function of the metal atom for a given ligand L goes in the order W < Cr < Mo. The high reactivity of Mo appears to be primarily an enthalpic effect, while the difference in reactivity between W and Cr is apparently primarily entropic in origin. For a given metal, the reactivity of a particular ligand is a function primarily of the geometry of the M(CO)$_5$(η^1-L) complex, with the complex requiring the least amount of rearrangement from the η^1 to the η^2 geometry being the one that isomerizes most rapidly. A competition between steric and electronic effects can be seen in the isomerization when L = 2-methyl-2,3-dihydrofuran (MeDHF). Even though the MeDHF complexes are more electron-rich than those of 2,3-DHF, for the Mo and W complexes, $\Delta H^‡$ is higher for isomerization of the MeDHF complexes. On the other hand, for the smaller Cr atom, $\Delta H^‡$ is lower for the MeDHF complex.

Thermodynamics. As with the reaction kinetics, the thermodynamics of the linkage isomerization depend on a balance between steric and electronic effects. We also find that entropic effects are very important in determining the equilibrium constant for a given M(CO)$_5$(L) system.

Acknowledgment. This work was supported by the Israel Science Foundation, founded by the Israel Academy of Arts and Sciences. We would also like to thank Dr. Pinchas Aped of the Bar-Ilan University Chemistry Department for assistance with the DFT calculations.

Supporting Information Available: Figures S-1 through S-4 (equilibrium data for Mo(CO)$_5$(L) and W(CO)$_5$(L)); Figure S-5 (time-resolved S^{2}FTIR spectra of the reaction between W(CO)$_5$-(CyH) and 1 mol L^{-1} 2,3-DHF); Figures S-6 and S-7 (additional views of the results of the DFT calculations); and Tables S-1 through S-6, listing the experimental values for k_{obs} and $\Delta A_\infty/\Delta A_0$ for reaction 1, and the values of K_{eq} and k_{12} derived therefrom. This material is available free of charge via the Internet at http://pubs.acs.org.

OM700456X

(25) Jones, W. D.; Dong, L.; Myers, A. W. *Organometallics* **1995**, *14*, 855.

(26) Booysen, J. F.; Bredenkamp, M. W.; Holzapfel, C. W. *Synth. Commun.* **1989**, *19*, 1437.

(27) (a) Chen, H.; Hodges, L. M.; Liu, R.; Stevens, W. C.; Sabat, M.; Harman, W. D., Jr. *J. Am. Chem. Soc.* **1994**, *116*, 5499. (b) Friedman, L. A.; Sabat, M.; Harman, W. D. *J. Am. Chem. Soc.* **2002**, *124*, 7395. (c) You, F.; Friedman, L. A.; Kimberley C. Bassett, K. C.; Lin, Y.; Sabat, M.; Harman, W. D. *Organometallics* **2005**, *24*, 2903.

(28) Goj, L. A.; Lail, M. A.; Pittard, K. A.; Riley, K. C.; Gunnoe, T. B.; Petersen, J. L. *Chem. Commun.* **2006**, 982.

(29) Breheny, C. J.; Kelly, J. M.; Long, C.; O'Keeffe, S.; Pryce, M. T.; Russell, G.; Walsh, M. W. *Organometallics* **1998**, *17*, 3690.

(30) The value of K_{eq} for W(CO)$_5$(2,5-DHF) was sufficiently high that we were able to place only a lower limit on its value and, hence, were not able to calculate $\Delta H°$ and $\Delta S°$ for the equilibrium.

(31) (a) Nechaev, M. S.; Rayón, V. M.; Frenking, G. *J. Phys. Chem. A* **2004**, *108*, 3134. (b) Cedeño, D. L.; Sniatynsky, R. *Organometallics* **2005**, *24*, 3882.

(32) While the DFT calculations appear to give fairly reliable structural information, they are not sufficiently accurate to give unambiguous energetic information about the various M(CO)$_5$(L) complexes. As shown in Table 4, the uncertainties in the calculated energetics of different systems are of similar magnitude to the differences between them, and in some cases, changing the basis set or functional can change the predicted value of $\Delta G°$ from negative to positive.